Fluorescently labeled human apurinic/apyrimidinic endonuclease APE1 reveals effects of DNA polymerase β on the APE1–DNA interaction

Artemiy S Bakman, Aleksandra A Kuznetsova, Lyudmila V Yanshole, Alexander A Ishchenko, Murat Saparbaev, Olga S Fedorova, Nikita A Kuznetsov

DNA Repair xxx (xxxx) 103450

Contents lists available at ScienceDirect

DNA Repair

journal homepage: www.elsevier.com/locate/dnarepair

Fluorescently labeled human apurinic/apyrimidinic endonuclease APE1 reveals effects of DNA polymerase β on the APE1–DNA interaction

Artemiy S. Bakman [a], Aleksandra A. Kuznetsova [a], Lyudmila V. Yanshole [b], Alexander A. Ishchenko [c], Murat Saparbaev [c, d], Olga S. Fedorova [a], Nikita A. Kuznetsov [a, e, *]

[a] Institute of Chemical Biology and Fundamental Medicine, Siberian Branch of Russian Academy of Sciences (SB RAS), 8 Prospekt Akad. Lavrentyeva, Novosibirsk 630090, Russia

[b] International Tomography Center SB RAS, 3a Institutskaya Str., Novosibirsk 630090, Russia

[c] Group "Mechanisms of DNA Repair and Carcinogenesis", Gustave Roussy Cancer Campus, CNRS UMR9019, Université Paris-Saclay, 94805 Villejuif, France

[d] NCJSC "Al-Farabi Kazakh National University" Almaty, Kazakhstan

[e] Department of Natural Sciences, Novosibirsk State University, 2 Pirogova Str., Novosibirsk 630090, Russia

ARTICLE INFO

Keywords:
DNA repair
Apurinic/apyrimidinic endonuclease
DNA-protein interaction
Protein-protein interaction
Damaged DNA transfer
Conformational change
Fluorescence
Pre-steady-state kinetics

ABSTRACT

The base excision repair (BER) pathway involves sequential action of DNA glycosylases and apurinic/apyrimidinic (AP) endonucleases to incise damaged DNA and prepare DNA termini for incorporation of a correct nucleotide by DNA polymerases. It has been suggested that the enzymatic steps in BER include recognition of a product–enzyme complex by the next enzyme in the pathway, resulting in the "passing-the-baton" model of transfer of DNA intermediates between enzymes. To verify this model, in this work, we aimed to create a suitable experimental system. We prepared APE1 site-specifically labeled with a fluorescent reporter that is sensitive to stages of APE1–DNA binding, of formation of the catalytic complex, and of subsequent dissociation of the enzyme–product complex. Interactions of the labeled APE1 with various model DNA substrates (containing an abasic site) of varied lengths revealed that the enzyme remains mostly in complex with the DNA product. By means of the fluorescently labeled APE1 in combination with a stopped-flow fluorescence assay, it was found that Polβ stimulates both i) APE1 binding to an abasic-site–containing DNA duplex with the formation of a catalytically competent complex and ii) the dissociation of APE1 from its product. These findings confirm DNA-mediated coordination of APE1 and Polβ activities and suggest that Polβ is the key trigger of the DNA transfer between the enzymes participating in initial steps of BER.

1. Introduction

Genomic DNA in the live cell constantly undergoes various molecular lesions due to endogenous and exogenous factors [1]. The most common type of DNA damage is a single-base lesion that involves the loss of a base through spontaneous hydrolysis [2], base oxidation [3–6], or alkylation [7–10] during physiological metabolism or modification by endogenous DNA-damaging agents. These types of DNA lesion are mutagenic and therefore are repaired in live cells. These lesions can arise both in single-stranded and in double-stranded DNA [11]. In the single-stranded DNA context, they can be repaired by homologous recombination [12,13] and template switching [14–16] mechanisms. By contrast, in double-stranded DNA, the single-base lesions are processed mainly by BER [17–21].

BER is a multistep process initiated by spontaneous or DNA glycosylase–initiated base loss. In the last case, DNA glycosylase recognizes and removes a damaged base, thereby generating an apurinic/apyrimidinic (AP) site [22,23]. Subsequently, the damaged DNA strand is incised by apurinic/apyrimidinic endonuclease 1 (APE1) on the 5′ side of the AP site to generate 3′-hydroxyl and 5′-deoxyribose phosphate (dRP) groups at the ends [24–27]. Then, DNA polymerase β (Polβ) adds a single nucleotide to the 3′-hydroxyl and removes the dRP group by means of intrinsic dRP lyase activity [28–32]. Alternatively, Polβ can insert 2–12 nucleotides thus creating a multinucleotide 5′-flap that is conse-

Abbreviations: αA, the α-anomer of 2′-deoxyadenosine; AP site, apurinic/apyrimidinic site; BER, base excision repair; DHU, 5,6-dihydrouridine; F, (2R,3S)– 2-(hydroxymethyl)– 3-hydroxytetrahydrofuran; FRET, Förster resonance energy transfer; SDS-PAGE, sodium dodecyl sulfate polyacrylamide gel electrophoresis

* Corresponding author at: Institute of Chemical Biology and Fundamental Medicine, Siberian Branch of Russian Academy of Sciences (SB RAS), 8 Prospekt Akad. Lavrentyeva, Novosibirsk 630090, Russia.

E-mail address: nikita.kuznetsov@niboch.nsc.ru (N.A. Kuznetsov).

https://doi.org/10.1016/j.dnarep.2023.103450
Received 24 August 2022; Received in revised form 26 December 2022; Accepted 9 January 2023
1568-7864/

quently cleaved off by flap endonuclease 1 (FEN1) [33,34]. The first subpathway including only single-nucleotide replacement is referred to as short-patch BER. Another subpathway including ≥ 2-nucleotide replacement and involving FEN1 for cleaving off the flap is called long-patch BER. At the final step of the BER pathway, the integrity of the DNA backbone is restored by a DNA ligase. Aside from the aforementioned repair enzymes, accessory proteins such as X-ray repair cross-complimenting protein 1 (XRCC1) [35–40], proliferating cell nuclear antigen (PCNA) [41,42], and poly(ADP-ribose) polymerase 1 (PARP1) [43] are believed to participate in the coordination of BER processes.

According to the "passing-the-baton" model of BER, DNA intermediates in BER are processed and then passed from one enzyme to another in a coordinated fashion [44–46]. Step-by-step coordination of BER events is thought to be facilitated by multiple protein–protein interactions comprising BER enzymes and accessory proteins [43,47–51]. Therefore, investigating not only protein–DNA but also protein–protein interactions is required for a complete understanding of the BER mechanism.

APE1 is one of BER enzymes that recognizes and incises a DNA strand containing an AP site [52,53]. Although the interaction of APE1 with DNA has been studied quite extensively, the interactions of this enzyme with other BER proteins and its participation in the coordination of BER processes are still debated. The last 2 decades saw a number of studies in this field: it has been found that APE1 stimulates catalytic activity of many human DNA repair glycosylases, including uracil DNA glycosylase (UNG) [54,55], thymine DNA glycosylase (TDG) [56–58], alkyladenine DNA glycosylase (AAG) [59,60], methyl-CpG-binding domain 4 (MBD4) [51], adenine DNA glycosylase MutY and MYH [61–64], and oxoguanine DNA glycosylase (OGG1) [51,65–68]. This effect has been explained: APE1 passively (not forming specific protein–protein interactions) and/or actively (forming specific interactions with glycosylase) displaces glycosylase from its complex with the product thereby raising the product-release rate of DNA glycosylase. This mechanism is still unclear and was discussed and clarified in recent and latest articles [68,69]. Besides, APE1 is reported to stimulate the dRP lyase activity of Polβ [70,71]. In turn, APE1 endonuclease activity is enhanced by some DNA glycosylases [50], Polβ [50,72], and XRCC1 [37,50,72]. The mutual enhancement of each other's enzymatic activities by APE1 and aforementioned proteins can materialize due to either direct [73,74] or DNA-mediated [51] protein–protein interactions. Indeed, it has been demonstrated that APE1 and DNA form ternary complexes with Polβ [70,75] and OGG1 [69]. The above data indicate that APE1 interacts with many other BER proteins, and further investigation is necessary to understand how exactly these proteins modulate each other's enzymatic activities to coordinate all BER processes.

A powerful tool for research into protein–protein interactions is a fluorescence-based approach, when a protein is labeled by a relatively small-molecule fluorescent dye. Such a fluorescently labeled protein can form natural contacts with DNA and other proteins, and the local environment of the fluorophore can thus change, leading either to alterations in own fluorescence intensity or to the formation of a Förster resonance energy transfer (FRET) pair with a quencher located in the partner molecule. Such an approach has been used to analyze direct protein–protein contacts in BER under equilibrium conditions [73] and revealed new features of APE1–OGG1 interactions in a recent work [69]. Thus, protein–protein and protein–DNA interactions can be monitored in real time by the measurement of the fluorescent signal via the stopped-flow technique under pre–steady-state conditions. Therefore, the aim of the present study was to create an experimental system based on fluorescently labeled APE1 that would allow us to analyze the protein–protein and protein–DNA interactions in BER. It turned out that the obtained labeled APE1 variants change fluorescence intensity when associating with DNA substrates containing an AP site thus enabling us to monitor kinetics of the enzyme–DNA interaction. It was revealed that Polβ specifically affects the interaction of APE1 with its substrate and its product. The mechanisms of these protein–protein interactions in BER are discussed at the end of the paper.

2. Materials and methods

2.1. Protein expression and purification

The wild type (WT) APE1 enzyme was expressed and purified as described previously [76]. Mutations C138S/C296S, C138S/C310S, and C296S/C310S were introduced into the pET11a-APE1 plasmid using a site-directed mutagenesis kit (QuikChange XL, Stratagene). For the expression of double mutants C138S/C296S, C138S/C310S, and C296S/C310S, 1 L of *Escherichia coli* strain Rosetta II(DE3) culture (Invitrogen, France) (in 2xYT broth) carrying the pET11a-APE1 construct was grown at 100 μg/mL ampicillin and 25 μg/mL chloramphenicol and 37 °C until absorbance at 600 nm (A_{600}) reached 0.6–0.7. APE1 expression was induced overnight with 0.5 mM isopropyl-β-D-thiogalactopyranoside at 25 °C. Purification of the mutant proteins was performed as described earlier [77,78].

Human DNA polymerase β (Polβ) was expressed in Rosetta 2 (DE3) *E. coli* cells. The cells carrying a pET28c expression vector were grown in 1 L of the Luria–Bertani (LB) medium supplemented with 50 μg/mL kanamycin at 37 °C to an optical density of 0.6 at 600 nm. Then, the temperature was lowered to 20 °C, and transcription was induced by the addition of 0.2 mM IPTG. After that, the cells were incubated for 16 h. The cells were harvested by centrifugation (5000 × *g*, 10 min) and then resuspended in a buffer (20 mM HEPES-KOH pH 7.8, 40 mM NaCl) followed by cell lysis by means of a French press. All the purification procedures were carried out at 4 °C. Each homogenate was centrifuged at 40,000 × *g* for 40 min, and the supernatant was passed through a column packed with 30 mL of the Q-Sepharose resin (Amersham Biosciences) pre-equilibrated in a buffer (20 mM HEPES-KOH pH 7.8, 200 mM NaCl). The flow-through fractions containing the Polβ protein were pooled, supplemented with 20 mM imidazole, and loaded on a 1 mL HiTrap-Chelating™ column (Amersham Biosciences). Bound proteins were eluted with a linear 20 → 500 mM gradient of imidazole.

The proteins' concentrations were measured by means of A_{280}; their stock solutions were stored at − 20 °C in 50 % glycerol.

2.2. Oligodeoxynucleotides

The sequences of the DNA and RNA substrates employed in this work are presented in Table 1. Oligodeoxynucleotides were synthesized by standard phosphoramidite methods on an ASM-800 synthesizer (BIOSSET Ltd., Novosibirsk, Russia) using phosphoramidites purchased from either Glen Research or ChemGenes. The synthetic oligodeoxynucleotides were purified by high-performance liquid chromatography on an Agilent 1200 chromatograph (USA) and a Zorbax SB-C18 column (5 μm), 4.6 × 150 mm, via a linear gradient of acetonitrile (0 → 50 %) in the presence of 20 mM triethylammonium acetate (pH 7.0) for 30 min at a flow rate of 2 mL/min. Fractions containing oligodeoxynucleotides were dried in vacuum, dissolved in water, and precipitated with 2 % $LiClO_4$ in acetone. After washing with pure acetone and drying, the oligodeoxynucleotide precipitates were dissolved in water and stored at − 20 °C until experiments. Concentrations of the oligodeoxynucleotides were determined through the use of A_{260}. Homogeneity of the purified oligodeoxynucleotides was evaluated by polyacrylamide gel electrophoresis in a denaturing 20 % gel. The oligodeoxynucleotides were visualized with the Stains-All dye (Sigma, USA). All DNA duplexes were prepared by annealing of modified and complementary strands at the 1:1 molar ratio in an aqueous solution.

Table 1
Sequences of oligodeoxynucleotides.[a]

Name	Sequence
F/G-13	5'-TCTCTC**F**CCTTCC-3'
	3'-AGAGAG**G**GGAAGG-5'
DHU/G-13	5'-TCTCTC(**DHU**)CCTTCC-3'
	3'-AGAGAG **G** GGAAGG-5'
αA/T-13	5'-TCTCTC(**αA**)CCTTCC-3'
	3'-AGAGAG **T** GGAAGG-5'
F/G-17	5'-GCTCA**F**GTACAGAGCTG-3'
	3'-CGAGT**G**CATGTCTCGAC-5'
F/G-3'BHQ-17	5'-GCTCA**F**GTACAGAGCTG-3'
	3'- **BHQ1**-CGAGT**G**CATGTCTCGAC-5'
F/G-5'BHQ-17	5'-GCTCA**F**GTACAGAGCTG-3'
	3'-CGAGT**G**CATGTCTCGAC-**BHQ1**-5'
C/G-3'BHQ-17	5'-GCTCA**C**GTACAGAGCTG-3'
	3'- **BHQ1**-CGAGT**G**CATGTCTCGAC-5'
C/G-5'BHQ-17	5'-GCTCA**C**GTACAGAGCTG-3'
	3'-CGAGT**G**CATGTCTCGAC-**BHQ1**-5'
U/G-17	5'-GCTCA**U**GTACAGAGCTG-3'
	3'-CGAGT**G**CATGTCTCGAC-5'
DHU/G-17	5'-TCTCTCTC(**DHU**)CCTTCCTT-3'
	3'-AGAGAGAG **G** GGAAGGAA-5'
FAM-F/G-17	5'-**FAM**-GCTCA**F**GTACAGAGCTG-3'
	3'-CGAGT**G**CATGTCTCGAC – 5'
FRET-F/G-17	5'-**FAM**-GCTCA**F**GTACAGAGCTG-3'
	3'-CGAGT**G**CATGTCTCGAC-**BHQ1**-5'
F/G-28	5'-GTGTCACCACTGCTCA**F**GTACAGAGCTG-3'
	3'-CACAGTGGTGACGAGT**G**CATGTCTCGAC-5'
FAM-F/G-28	5'-**FAM**-GTGTCACCACTGCTCA**F**GTACAGAGCTG-3'
	3'-CACAGTGGTGACGAGT**G**CATGTCTCGAC-5'

[a] FAM is 6-carboxyfluorescein, BHQ1 is black hole quencher, FRET is Förster resonance energy transfer, F is (2 *R*,3 *S*)– 2-(hydroxymethyl)– 3-hydroxytetrahydrofuran [a reduced analog of an AP (abasic) site], DHU is 5,6-dihydrouridine, and αA is the α-anomer of 2′-deoxyadenosine.

2.3. Protein labeling

Fluorescent labeling of APE1 was implemented by incubation of a protein (50 μM) with a fivefold molar excess of Alexa Fluor™ 488 C5 maleimide (Thermo Fisher Scientific) for 3 h at 4 °C in labeling buffer (50 mM HEPES/KOH pH 7.4, 25 mM NaCl). The unincorporated free dye was then removed using a 3 kDa Amicon centrifugal filter (Merck, Germany). Final concentrations of the protein and incorporated label were determined by measurement of A_{280} and A_{491} with the help of corresponding extinction coefficients for APE1 and Alexa Fluor 488. The labeled proteins were subjected to SDS-PAGE analysis, and the gels were visualized by fluorescence analysis to monitor the dye label and by Coomassie Blue staining to monitor the protein. The number of dye molecules attached to an APE1 molecule was determined by matrix-assisted laser desorption ionization time-of-flight (MALDI-TOF) mass spectrometry. Based on these data and on literature data about sites of APE1 modification [69,79], the labeling sites were chosen for our cases.

2.4. Polyacrylamide gel electrophoresis analysis of DNA cleavage by labeled proteins

To verify the AP endonuclease activity of labeled APE1, polyacrylamide gel electrophoresis analysis of cleavage was performed using a substrate called FAM-F/G-17 (Table 1). To start a reaction between the enzyme and substrate, their solutions were mixed at 25 °C in reaction buffer, which was composed of 50 mM Tris-HCl pH 7.5, 50 mM KCl, 6 mM $MgCl_2$ 1 mM EDTA, and 7 % of glycerol (v/v), with final protein and DNA concentrations of 0.05 and 1 μM, respectively. After 20 s from its start, the reaction was quenched by means of a gel loading dye containing 8 M urea and 25 mM EDTA. The obtained samples were then loaded on a 20 % (w/v) polyacrylamide/7 M urea gel. The gels were visualized using an E-Box CX.5 TS gel-documenting system (Vilber Lourman, France) and quantified in the Gel-Pro Analyzer software (Media Cybernetics, Rockville, MD).

2.5. Mass-spectrometric analysis

These experiments were conducted at the multiaccess center Mass-Spectrometric Investigations (SB RAS, Novosibirsk, Russia) on a MALDI-TOF/TOF Ultraflex III mass spectrometer (Bruker Daltonics, Germany). Proteins were identified by this mass-spectrometric analysis. Each sample was precipitated with 9 volumes of cold acetone (−20 °C), and the pellet was dissolved and incubated in 10 μL of 8 M urea/0.4 M AmB buffer at 60 °C for 1 h. After cooling of the samples to room temperature, 50 μL of 40 mM AmB buffer containing sequencing-grade modified trypsin (1 μg trypsin per 50 μg protein) was added to the mixture to attain 2 M urea concentration. The digestion reactions were allowed to proceed for 16 h at 37 °C. Peptides were desalted using C18 ZipTips (Millipore), mixed (at 0.5 μL of the sample per 0.5 μL of the matrix) with 2,5-dihydroxybenzoic acid dissolved in a 70 % acetonitrile/0.1 % trifluoroacetic acid mixture, and spotted onto a standard MTP ground steel plate (Bruker Daltonics). The mass spectra of the tryptic protein digests were recorded in reflective positive ion mode in the *m/z* range of 350–4700. The spectra were next analyzed in the FlexAnalysis software (v3.0, build 96, Bruker Daltonics), and peptide masses were entered into local MASCOT server 2.2.04 for the identification of peptides.

2.6. Stopped-flow fluorescence assays

Stopped-flow measurements with fluorescence detection were carried out mostly as described previously [80–82] by means of a model SX.20 stopped-flow spectrometer (Applied Photophysics Ltd., UK). Fluorescence of Alexa Fluor 488 was excited at λ_{ex} = 495 nm and monitored at λ_{em} > 530 nm (with Schott filter OG-530). Typically, each trace shown is the average of four or more individual experiments. Usually, the experiments were conducted at 25 °C in reaction buffer consisting of 50 mM Tris-HCl pH 7.5, 50 mM KCl, 1.0 mM EDTA, 6.0 mM $MgCl_2$, and 7 % of glycerol (v/v). Nonetheless, when we investigated only protein–DNA binding without DNA cleavage, we used the binding buffer that did not contain $MgCl_2$ but contained 10 mM EDTA to prevent AP endonuclease activity of APE1. Such experimental cases without Mg^{2+} are marked specially. All reported concentrations represent the final concentration of components after mixing.

The stopped-flow curves were fitted to the double-exponential equation

$$F = F_0 + F_1\,(1 - \exp(-k_1 t)) + F_2\,(1 - \exp(-k_2 t)), \quad (1)$$

where F is the observed fluorescence, F_0 is the background fluorescence, $F_1$and F_2 are fluorescence parameters, and k_1 and k_2 are the observed rate constants of the first and the second stages, respectively.

2.7. A microscale thermophoresis (MST) assay

Binding of the APE1 enzyme–substrate complex to Polβ was determined via the MST approach on a Monolith NT.115 instrument (NanoTemper Technologies, Germany). In all titration experiments, the concentrations of labeled APE1 C138S/C296S and F/G-28 (i.e., [APE1] and [F/G-28]) were 0.5 μM, and concentrations of Polβ were varied from 0.02 to 30.00 μM. The reaction mixtures were incubated at 25 °C in binding buffer consisting of 50 mM Tris-HCl pH 7.5, 50 mM KCl, and 10 mM EDTA.

To fit the MST data, we used the model in which one molecule of the APE1–DNA complex binds to one molecule of Polβ to form a ternary complex:

$$APE1\frac{F}{G}-28+Pol\beta \rightleftharpoons APE1\frac{F}{G}-28Pol\beta$$

The dissociation constants were calculated with the help of the following equation derived from the above model:

$$MST\,signal = F_1 + (F_2 - F_1) \times \left(\frac{\left(K_d + [Pol\ \beta]_t + [APE\ 1]_t\right) - \sqrt{\left(\left(K_d \right.\right.}}{2[}$$

where K_d is the dissociation constant, $[Pol\beta]_t$ is the total Polβ concentration, $[APE1]_t$ is the total APE1 concentration, F_1 is the signal of APE1–F/G-28 without added Polβ, and F_2 is the signal at the maximal Polβ concentration.

2.8. An electrophoretic mobility shift assay

Binding reactions were prepared at room temperature in the following reaction buffer: 50 mM Tris-HCl pH 7.5, 50 mM KCl, 6 mM $MgCl_2$, 1.0 mM DTT, 1.0 mM EDTA, and 7 % of glycerol. Concentration of fluorescently labeled DNA FAM-F/G-28 (Table 1) was 40 nM in all the samples. Concentration of APE1 was 80 nM if it was added, and Polβ concentration was varied from 0 to 1000 nM. Reaction mixtures were incubated for 5 min before loading onto a 10 % native gel (acrylamide:bisacrylamide, 37.5:1.0) at 4 °C. The gel was equilibrated and subjected to an electrophoretic pre-run at 4 °C for at least 30 min before the samples were loaded. After that, the gel was subjected to electrophoresis at 150 V for 90 min in 0.5 TBE and scanned on a VersaDoc gel imaging system.

3. Results and discussion

3.1. Alexa Fluor 488 labeling of APE1

Recently, three Cys residues of APE1 (Cys138, Cys296, and Cys310) were found to be labeled by an iodoacetamide-based chemical modification agent [79]. Accordingly, we prepared three APE1 double mutants—C138S/C296S, C138S/C310S, and C296S/C310S—expecting that each mutant enzyme would be labeled only at one site. In this work, we utilized Alexa Fluor 488 C5 maleimide to label the WT and aforementioned double mutants of APE1. After labeling followed by the removal of the unincorporated reagent, optical spectra were recorded to estimate the ratios of the protein to the attached fluorophore (Supplementary Fig. S1). It was proved that the concentration of Alexa Fluor 488 is higher than the protein concentration for all the samples (Supplementary Table S1). To verify that the unincorporated label is completely removed from the samples, SDS-PAGE with visualization by fluorescence and Coomassie Blue staining was performed (Supplementary Fig. S2). It was demonstrated that Alexa Fluor 488 is attached to the proteins, and that the samples are devoid of the free label. After that, MALDI mass spectra revealed that WT and C296S/C310S APE1 are mainly doubly labeled, whereas C138S/C296S APE1 is mainly labeled at the single site (Supplementary Figs. S3–S6), indicating that the label was attached to Cys138 and to some other residue. These findings are in agreement with electronic absorption spectra showing labeling efficiency of ~2 for WT and C296S/C310S but 1.4 and 1.3 for C138S/C310S and C138S/C296S, respectively (Supplementary Table S1).

In the latest work [69], it was shown that the Cys99 residue also can be labeled by a maleimide-based reagent. Therefore, to determine the labeling sites in APE1, MALDI mass spectra were obtained for trypsin digestion products of labeled and unlabeled APE1 (Supplementary Fig. S7). It was determined that in the case of a labeled protein, in the MALDI mass spectra, there is a peak at m/z 2831.8 corresponding to the peptide "amino acid residues 86–103" conjugated with the Alexa Fluor 488 label, thus confirming the attachment of the dye to the Cys99 residue.

Therefore, these results suggested that in our case, APE1 mostly gets labeled on residues Cys138 and Cys99 or only on Cys99 in the cases of mutants C138S/C310S and C138S/C296S. Indeed, the elimination of Cys138 substantially reduced the labeling efficiency of APE1, whereas the elimination of residues Cys296 and Cys310 did not have any noticeable effect on labeling efficiency in comparison with WT APE1. For subsequent experiments, we prepared C138S/C296S APE1 labeled mainly at the Cys99 residue and WT and C296S/C310S APE1 that are labeled mainly at Cys99 and Cys138. Polyacrylamide gel electrophoresis analysis of the AP endonuclease activity revealed that free double mutants as well as Alexa Fluor 488–labeled APE1 enzymes retain the activity of WT APE1 (Supplementary Fig. S8).

All the four sites of labeling of APE1 on Cys are illustrated in Fig. 1, which depicts the structure of DNA-bound APE1. The analysis of APE1 structure suggested that Cys99 and Cys138 are the most sterically accessible for the testing of our hypothesis about labeling sites. It was obvious that Cys99 and Cys310 are close to the DNA-binding site, whereas Cys138 and Cys296 are located at a distance on the other side of the protein molecule. Taking into account these findings, changes in Alexa Fluor 488 fluorescence intensity during APE1 interaction with DNA were analyzed as a function of the distance between the Cys99 residue and BHQ1 quencher labels attached to DNA.

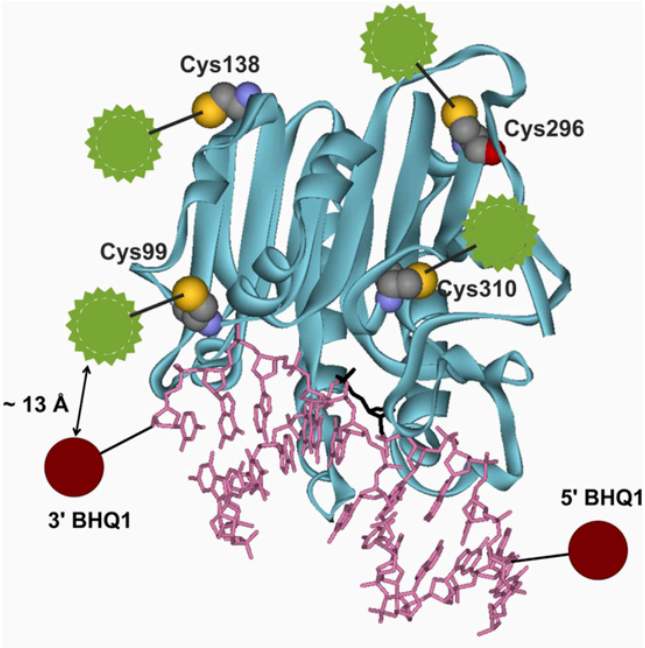

Fig. 1. Crystal structure of APE1 bound to AP site–containing DNA (PDB code: 1DE8) with four Cys residues known to be labeled according to the literature. The fluorescent label is schematically pictured in the green color. The BHQ1 quencher residue attached at the 3′ or 5′ end of the model DNA duplexes is shown too. The damaged nucleotide is highlighted in black. The estimated distance between the Cys99 residue and 3'BHQ1 is 13 Å, which is shown in the figure. Estimation of this and other distances between fluorophores on Cys residues and fluorescence quenchers on DNA is shown in Supplementary Fig. S9 and Supplementary Table S2. (For interpretation of the references to color in this figure legend, the reader is referred to the web version of this article.)

3.2. The stopped-flow assay of the interaction of labeled APE1 with 17-nt duplex oligodeoxynucleotides

When labeled C138S/C296S APE1 was mixed with an undamaged intact DNA duplex containing the BHQ1 quencher at the 3′ or 5′ end of the duplex (Table 1, C/G-3'BHQ-17 and C/G-5'BHQ-17), there was a barely noticeable decrease in Alexa Fluor 488 fluorescence intensity in the initial part of kinetic curves (Fig. 2 A). On the contrary, when the labeled C138S/C296S APE1 was mixed with one of F-site–containing 17-nt duplex oligodeoxynucleotides (Table 1), two-phase fluorescence curves were registered, supporting the notion that a specific enzyme–substrate interaction was reflected by Alexa Fluor 488 fluorescence.

Unexpectedly, the interaction of APE1 with unlabeled duplex F/G-17 also caused the growth of fluorescence intensity of the dye. This effect can be explained by the assumption that specific binding of DNA in the active site of the enzyme induces the replacement of the dye residue on the enzyme surface and an alteration of the fluorophore's local environment, resulting in an increase of the fluorescence intensity. In fact, in the crystal structure of the enzyme–substrate complex (Fig. 2), the site of fluorophore attachment (Cys99) is very close to the DNA sugar-phosphate backbone (the distance is ~7 Å). Hence, it seems possible that specific binding of DNA by labeled APE1 causes an alteration in the fluorophore's local environment. Of note, when APE1 interacted with F/G-5'BHQ-17, the first phase was fluorescence growth as in the case of unlabeled DNA; by contrast, a fluorescence decrease was seen when APE1 interacted with F/G-3'BHQ-17, suggesting that the BHQ1 that is attached at the 3′ end can efficiently quench Alexa Fluor 488 at the early step of the interaction. The second phase was a decrease in the fluorescence for all three types of model DNA duplexes containing an AP site. The curves were fitted to double-exponential Eq. 1, and observed rate constants for both phases were determined (Table 2).

Pre–steady-state kinetics of the interaction of APE1 with F-site–containing DNA have been previously studied via monitoring of intrinsic Trp fluorescence of the protein [76,83,84] and of FAM fluorescence in the substrate called FRET-F/G-17 (Table 1) [85]. Therefore, the obtained Alexa Fluor 488 fluorescence curves could be interpreted by their comparison with previously described Trp and FAM fluorescence curves for the same process (Fig. 2B, Table 2). The comparison revealed that the first phase of Alexa Fluor 488 fluorescence curves corresponds to the first phase of the Trp and FAM fluorescence traces; this phase was attributed to the enzyme–DNA binding and to the formation of a catalytically competent complex, in accordance with our previous findings [83,84,86,87]. These results indicate good agreement among intramolecular conformational changes of the enzyme (own Trp residues of enzyme), intramolecular changes of the DNA duplex (FRET detection of the FAM/BHQ1 pair in model DNA), and the intermolecular association detected by the fluorophore and quencher attached to the enzyme and DNA, respectively.

The second phase of the Alexa Fluor 488 fluorescence traces (a decrease in all cases between time points "0.02 s" and "5 s") matches fluorescence growth in the Trp and FAM curves (Fig. 2B), which was previously ascribed to DNA cleavage and product release steps [78,84–87]. It is worth noting that the stopped-flow fluorescence approach cannot monitor the cleavage of the DNA phosphodiester bond directly. Using this approach, we can monitor only some conformational rearrangements after the cleavage step. Consequently, here we cannot kinetically separate DNA cleavage and some product release steps; thus, we believe that the second phase of the fluorescence traces corresponds to both of these steps together. This phenomenon could cause the discrepancy between the DNA cleavage rate constants obtained by us and those determined by the rapid quench flow technique [88,89]. Indeed, this technique allows to find the "real" rate of hydrolysis if the rate of the quenching reaction is faster than the rate of APE1's cleavage reaction.

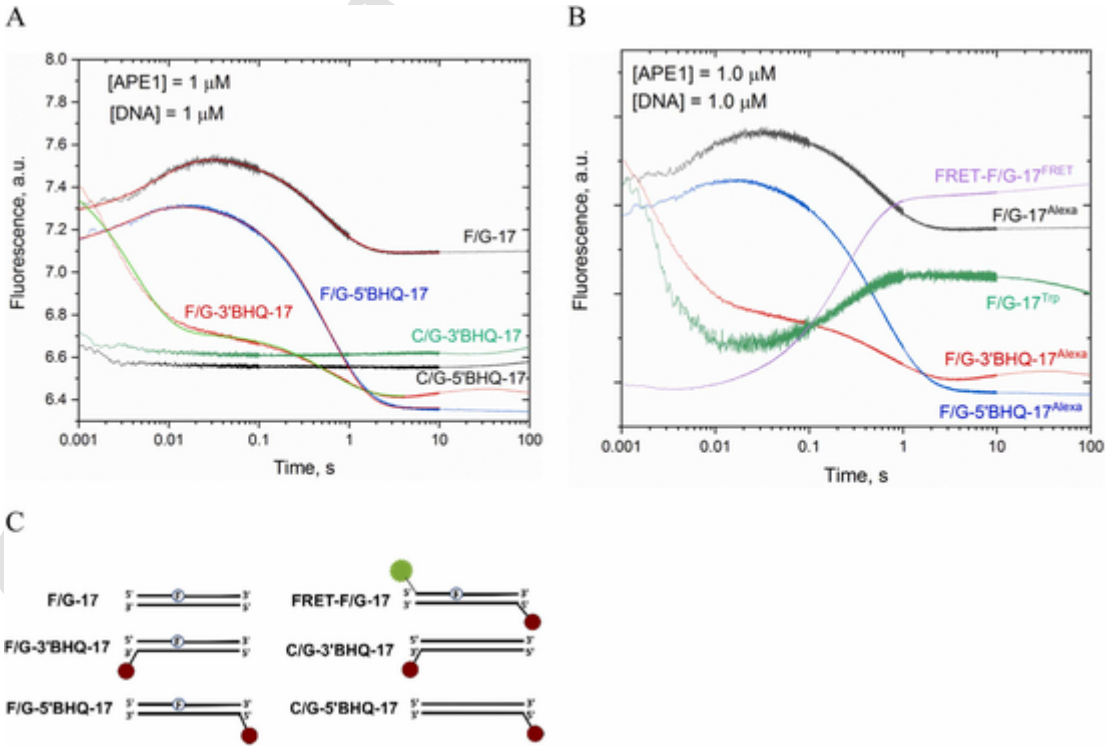

Fig. 2. (A) Changes in Alexa Fluor 488 fluorescence during the interaction of labeled C138S/C296S APE1 with one of F-site–containing 17-nt duplex oligodeoxynucleotides or intact 17-nt duplex oligodeoxynucleotides. Experimental data and results of the double-exponential fitting (Eq. 1) are presented as jagged and smooth traces, respectively. (B) Alexa Fluor 488 fluorescence traces of labeled C138S/C296S APE1 interacting with a 17-nt F-site–containing duplex oligodeoxynucleotide (F/G-17, F/G-3'BHQ-17, or F/G-5'BHQ-17; Table 1) in comparison with FRET-signal traces of the substrate called FRET-F/G-17 interacting with unlabeled APE1 [85] and Trp fluorescence traces of unlabeled APE1 interacting with F/G-17 [76,83,84]. (C) Schematics of the DNA substrates.

Table 2
The observed rate constants of the interaction of APE1 with each F-site–containing oligodeoxynucleotide, as calculated from the Alexa Fluor 488, FAM, and Trp fluorescence traces.

Fluorophore	Substrate	k_1, s^{-1}	k_2, s^{-1}
Alexa Fluor 488 in the protein	F/G-3'BHQ-17	246 ± 1	1.64 ± 0.04
	F/G-5'BHQ-17	262 ± 3	1.66 ± 0.01
	F/G-17	127 ± 1	1.84 ± 0.02
FAM/BHQ1 FRET pair in oligodeoxynucleotide	FRET-F/G-17	500 ± 80	4.08 ± 0.01
Trp residues in protein	F/G-17	407 ± 3	3.92 ± 0.02

Therefore, the discrepancy between the two methods can be attributed to these features of reaction step detection by each method. It is worth noting that the DNA cleavage assay performed previously by our group [86] yielded data consistent with stopped-flow cleavage rates derived in the present study.

In the experiments with F/G-17 and F/G-5'BHQ-17, fluorescence intensity of Alexa Fluor 488 tended to return to the initial level, possibly indicating dissociation from the product. By contrast, in the case of F/G-3'BHQ-17, the second decrease in Alexa Fluor 488 fluorescence intensity was unexpected because the product release should return the enzyme to its DNA-free state and abrogate the quenching effect of BHQ1. Therefore, we concluded that the dissociation of the enzyme–product complex consists of several stages. The proposed stages of the full enzymatic cycle of the APE1–DNA interaction monitored via the Alexa Fluor 488 fluorescence changes are outlined in Fig. 3. The product dissociation is started by an initial fast release of a short 5-nt oligodeoxynucleotide from the 5′ end of the F-site–containing DNA strand. On the other hand, the complex of APE1 with the other part of the DNA product, which contains the BHQ1 quencher, is quite stable (Fig. 3A). This partial dissociation can alter the local environment of the fluorophore attached to Cys99. Indeed, the Cys99 residue is positioned in the part of DNA duplexes that is affected by such partial dissociation (Fig. 1). Apparently, further dissociation of the enzyme–product complex proceeds only to a small extent. Perhaps the small amplitude of fluorescence growth from second 3 to second 30 in the F/G-3'BHQ-17 curve can be attributed to this step (Fig. 3B).

It is known that APE1 can recognize and cleave also DNA duplexes containing 5,6-dihydro-2′-deoxyuridine (DHU) [90] or 2′-deoxyuridine (U) [91]. Consequently, we recorded stopped-flow fluorescence curves for the interaction of labeled C138S/C296S APE1 with substrates U/G-17 and DHU/G-17 (Supplementary Fig. S10A). The results indicated that the initial phase that matched the formation of the enzyme–DNA complex was not detectable for DNA substrates containing damaged bases. This observation suggested that the mechanism and efficiency of recognition of such damaged nucleotides differ from those of a substrate containing an F-site, as reported earlier [92]. Despite these observations, in DHU/G-17's curve, a fluorescence decrease phase from second 5 to second 200 was documented here, which could be attributed to the DNA cleavage.

We also recorded fluorescence traces of the interaction of labeled WT APE1 or of labeled APE1 mutants with 17-nt F-site–containing duplex oligodeoxynucleotides (Supplementary Fig. S10B and S10C). It was demonstrated that all the fluorescence curves obtained using all the versions of labeled APE1 are almost identical, with a difference mainly in amplitudes of the changes. The similarity of the fluorescence traces obtained with the different labeled APE1 proteins suggested that only the Cys99-attached label, which is present in all the tested proteins, undergoes considerable changes in fluorescence during the enzyme–DNA interaction.

3.3. The interaction of labeled APE1 with F-site–containing duplex oligodeoxynucleotides of different lengths

Stopped-flow fluorescence traces were recorded for the interaction of labeled C138S/C296S APE1 with F-site–containing 13-nt (F/G-13) and 28-nt (F/G-28) DNA duplexes. The resultant Alexa Fluor 488 fluorescence curves have an initial phase of fluorescence growth and a subsequent fluorescence decrease phase, just as the curve for F/G-17 does (Fig. 4 A). Therefore, we successfully detected the enzyme–substrate

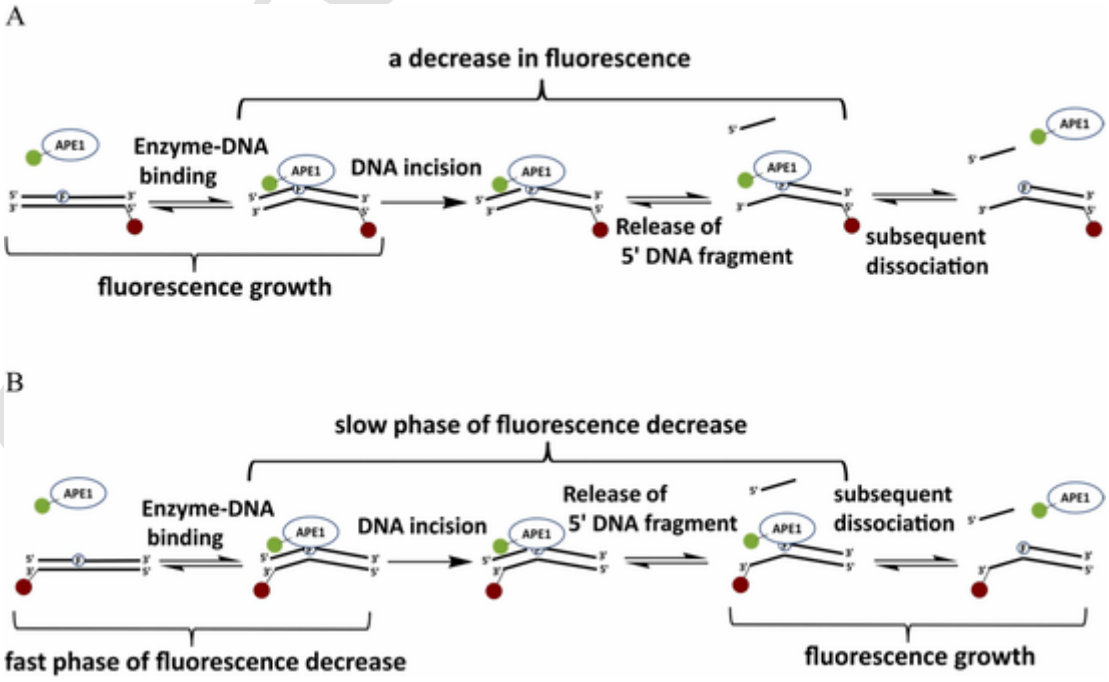

Fig. 3. Schematic representation of individual steps of the interaction of APE1 with F/G-17 or F/G-5'BHQ-17 (A) or F/G-3'BHQ-17 (B) as monitored via Alexa Fluor 488 fluorescence intensity changes.

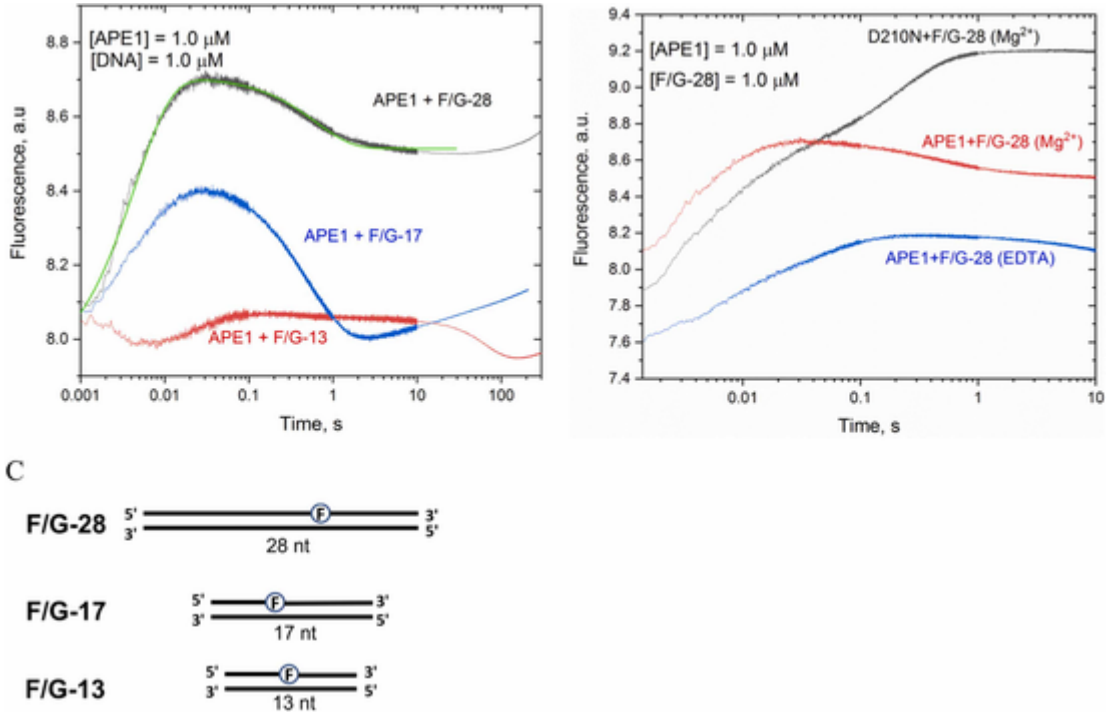

Fig. 4. (A) Alexa Fluor 488 fluorescence traces of the interaction of labeled C138S/C296S APE1 with the 13-nt (F/G-13), 17-nt (F/G-17), or 28-nt (F/G-28) duplex oligodeoxynucleotide containing an F-site. The smooth green curve is the double-exponential fit (Eq. 1) of the corresponding experimental curve. (B) Alexa Fluor 488 fluorescence traces of the interaction of labeled D210N APE1 with F/G-28, and fluorescence traces of the interaction of labeled C138S/C296S APE1 with F/G-28 in the presence of $MgCl_2$ (Mg^{2+}) or without Mg^{2+} (with EDTA). (C) Schematics of the DNA substrates. (For interpretation of the references to color in this figure legend, the reader is referred to the web version of this article.)

complex formation and product release after DNA cleavage for the DNA substrates of different length. In the case of the 13-nt duplex, however, the fluorescence changes had very small amplitude, making this DNA substrate a poor model for studying the enzyme–DNA interactions. In the case of the 28-nt duplex oligodeoxynucleotide, the fluorescence curve was similar to that of F/G-17. On the other hand, it was evident that in contrast to the F/G-17 fluorescence curve, in the F/G-28 curve, the final fluorescence level is much higher than the level of initial fluorescence (at ~1 ms). Such small amplitude for the phase of the fluorescence decrease indicated that the enzyme–product complex dissociates poorly in the case of F/G-28, and most of APE1 molecules remain in complex with the cleaved DNA after the reaction, in good agreement with earlier reports [83,93–95]. In addition, for F/G-28, we do not expect the decomposition of the nicked DNA duplex as in the case of F/G-17 (Fig. 3) because the 11-nt and 16-nt oligodeoxynucleotides obtained after F/G-28 cleavage are quite stable in the duplex state, in contrast to the 5-nt oligodeoxynucleotide obtained after the cleavage of F/G-17. The double exponential fit (Eq. 1) of the fluorescence trace of the interaction between APE1 and F/G-28 (Fig. 4 A) yielded the rate constants $k_1 = 224 \pm 1\ s^{-1}$ and $k_2 = 1.60 \pm 0.01\ s^{-1}$ for initial growth and the subsequent decrease of fluorescence, respectively. The proposed stages of the interaction between APE1 and F/G-28 as monitored via the Alexa Fluor 488 fluorescence changes are schematically displayed in Fig. 5.

We also registered stopped-flow fluorescence curves of the interaction of the labeled APE1 with 13-nt duplexes containing either DHU (DHU/G-13) or αA (αA/T-13) (Supplementary Fig. S11). There were no appreciable fluorescence changes on the curves obtained for these substrates, meaning that the binding of short 13-nt substrates of nucleotide incision repair also considerably differs from the binding of an F-site–containing duplex oligodeoxynucleotide.

3.4. Effects of Mg^{2+} and of the D210A mutation on the interaction of APE1 with F-site–containing duplexes

It is known that the absence of Mg^{2+} [85]—just as substitution D210N [87]—inactivates APE1. Therefore, in order to study only the binding of APE1 to F-site–containing duplex oligodeoxynucleotides (without the cleavage reaction), we prepared reaction buffer containing 10 mM EDTA to eliminate Mg^{2+} from the bulk solution, and we labeled catalytically inactive mutant D210N APE1 with Alexa Fluor 488. The fluorescence traces observed in these settings are presented in Fig. 4B. Both on the curves for apo-APE1 (without Mg^{2+}) and on the curves of

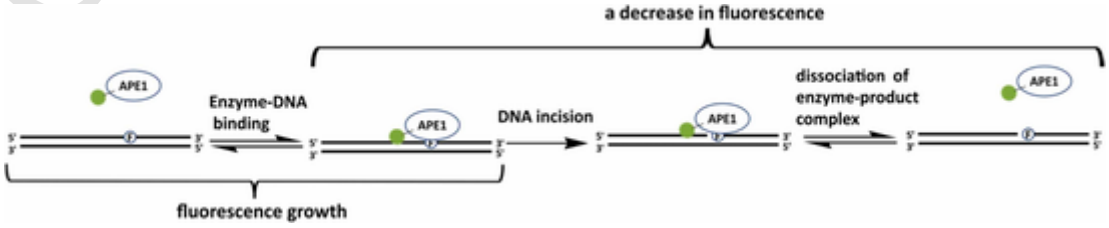

Fig. 5. Schematic representation of individual steps of the interaction of APE1 with F/G-28 as monitored by means of changes in Alexa Fluor 488 fluorescence intensity.

catalytically inactive D210N APE1, we detected the DNA-binding step, which enhanced fluorescence intensity.

Readers can see that the fluorescence trace for D210N + F/G-28 (Mg^{2+}) has some differences from that for APE1 + F/G-28 (EDTA) (Fig. 4B). Firstly, the trace for D210N + F/G-28 (Mg^{2+}) has two clearly separated phases of fluorescence growth. Indeed, it has been shown previously by our group that APE1 binding to its substrate proceeds in two steps, but we could not register these two steps separately under all experimental conditions [86,87,96]. Often, when one of these steps is much faster than the other one, we can monitor only the slower step. It has been reported previously that Mg^{2+} ions affect the second step of the enzyme-substrate binding [85]. This finding can explain the difference between these fluorescence traces. Moreover, the trace for D210N + F/G-28 (Mg^{2+}) has larger amplitude and longer time to reach the plateau. The difference in the amplitude is explained by a difference in binding affinity for a DNA substrate between WT APE1 and the D210N mutant, as demonstrated by our group [87] and others [88]. Furthermore, we have previously shown that the binding rate constant for D210N APE1 is less than the one for WT APE1 [87] thereby explaining the difference in plateau-reaching time between our fluorescence curves.

3.5. The interaction of labeled APE1 with Polβ

Previously, a strong binding of FAM-labeled APE1 to Polβ with a half-maximal effective concentration of 84 ± 7 nM has been reported [73]. By contrast, in another work, a direct interaction between APE1 and Polβ in the absence of DNA could not be detected by an analytical ultracentrifugation assay [97]. To visualize direct binding of APE1 to Polβ, we attempted to monitor changes of Alexa Fluor 488–labeled APE1 during its interaction with unlabeled Polβ in real time by the stopped-flow fluorescence assay (Supplementary Fig. S12). It was revealed that Alexa Fluor 488 fluorescence intensity does not change in the course of direct APE1–Polβ protein–protein interaction. It is possible that the position of labeled Cys99 is close to the DNA-binding site and quite distant from the surface that interacts with Polβ. Indeed, as reported in a recent study [50], potential contacts between APE1 and Polβ are far away from Cys99.

Therefore, we examined a DNA-mediated interaction between APE1 and Polβ using substrate F/G-28 because this duplex is large enough to accommodate both enzyme molecules. First, we mixed labeled C138S/C296S APE1 with F/G-28 in binding buffer (EDTA, without Mg^{2+}) to prevent DNA cleavage by APE1. After that, the resultant APE1–DNA complex was rapidly mixed with Polβ (in the same binding buffer) by the stopped-flow apparatus with continuous Alexa Fluor 488 fluorescence monitoring. The obtained fluorescence curve indicated the growth of fluorescence up to time point 0.1 s (Fig. 6 A). A similar curve was obtained for labeled D210N APE1 in the reaction buffer containing Mg^{2+}. At the same time, the control curve (when the APE1–DNA complex was mixed with the buffer) did not show any meaningful changes in fluorescence. Thus, the Cys99-labeled enzyme allows us to monitor the specific DNA-mediated interaction between APE1 and Polβ.

Because it was determined that the growth of Alexa Fluor 488 fluorescence in the stopped-flow curves corresponds to the binding of APE1 to an F-site–containing oligodeoxynucleotide and formation of a catalytically competent complex, we can propose that Polβ stimulates these steps of APE1 enzyme–substrate interaction. Such stimulation may be mediated by the assembly of the ternary complex: APE1–DNA–Polβ. Indeed, such a complex of DNA containing an uncleaved AP site, of APE1, and of Polβ has been detected by an electrophoretic mobility shift assay [70]. Additionally, we performed the MST assay, which revealed the binding between the APE1–F/G-28 complex (in EDTA buffer) and Polβ with estimated dissociation constant K_d = 2.5 ± 0.8 μM (Fig. 6B).

Next, we assessed the interaction between Polβ and the complex of APE1 with the cleaved DNA product. For this purpose, labeled C138S/C296S APE1 was mixed with F/G-28 in reaction buffer containing Mg^{2+} and incubated for 5 min to generate the cleaved DNA product. As demonstrated above, after this reaction, labeled APE1 remains in the complex with cleaved DNA. Then, the resultant enzyme–product complex of labeled APE1 was rapidly mixed with Polβ by the stopped-flow apparatus. The fluorescence curve showed a dramatic fluorescence decrease until second 1 (Fig. 6 C). Although the control curve without Polβ also contains some decrease in fluorescence intensity, its amplitude is much less than that of the curve with Polβ. Because the labeled APE1 in the complex with cleaved F/G-28 manifested greater fluorescence intensity than DNA-free labeled APE1 did (as illustrated in Fig. 4 A), the decrease in fluorescence intensity can be explained by the dissociation of APE1 from the DNA product. For instance, in the control curve, we noticed small partial dissociation of APE1 from its product as a consequence of dilution after stopped-flow mixing with the buffer. To strengthen this conclusion, we also performed an electrophoretic mobility shift assay where we added Polβ at different concentrations to F/G-28 and catalytically active APE1 (Supplementary Fig. S13). This assay revealed that the increase in Polβ concentration leads to the enhancement of the band corresponding to the Polβ–DNA complex. Despite we did not see Polβ-dependent decrease in the amount of APE1-DNA complex in the gel in the electrophoretic mobility shift assay, the disappearance of the band corresponding to APE1's enzyme–product complex at the highest concentration of Polβ (1 μM) was observed.

The Polβ-induced APE1 dissociation from its product is consistent with the passing-the-baton model of BER, according to which, Polβ should recognize the complex of APE1 with cleaved DNA and displace APE1 from it. Possibility of the recognition of the complex of APE1 with cleaved DNA by Polβ has been revealed by electrophoretic mobility shift assay–based detection of the ternary complex of APE1, cleaved DNA, and Polβ [75].

Thus, our data revealed that Polβ affects the APE1–DNA interaction in two ways. Firstly, Polβ stimulates the binding of APE1 to its substrate thereby promoting the assembly of a catalytically competent complex. Secondly, Polβ stimulates the release of the cleaved DNA product from its complex with APE1. Both effects lead to the stimulation of APE1's general AP endonuclease activity by Polβ, as reported previously [50].

A number of studies have been conducted to understand functions of APE1's N-terminal domain during interactions with DNA, RNA, and some proteins [37,72,98–101]. APE1's N-terminal domain has been shown to be critical for the interaction of APE1 with nucleophosmin (NPM1) [98,99], XRCC1 [37], and some DNA glycosylases [100]. Nevertheless, the involvement of the N-terminal extension of APE1 in the interaction with other canonical BER proteins remains unexplored [72]. It has been demonstrated that the absence of APE1's first 33 amino acid residues significantly enhances the rate of AP endonuclease reaction [99]. Based on this finding, it was stated that the N-terminal domain precludes APE1 from fast dissociation from the AP endonuclease product. On the other hand, this notion contradicts findings of another study, which did not show such enhancement of the AP endonuclease reaction rate when APE1's N-terminal domain is absent [100]. Thus, the role of the N-terminal domain of APE1 in the regulation of BER should be studied further.

To clarify the role of APE1's N-terminal domain in the interaction with Polβ, we isolated and fluorescently labeled the APE1 mutant lacking the first 34 N-terminal residues and having the D210N amino acid substitution (Δ34-D210N-APE1). The experiments on AP DNA substrate–mediated interaction with Polβ did not reveal significant change in the strength of this interaction compared to full-length D210N APE1 (Supplementary Fig. S14A). This result is consistent with a study indicating that APE1's N-terminal domain only slightly affects both the direct and the DNA-mediated interactions with Polβ [72].

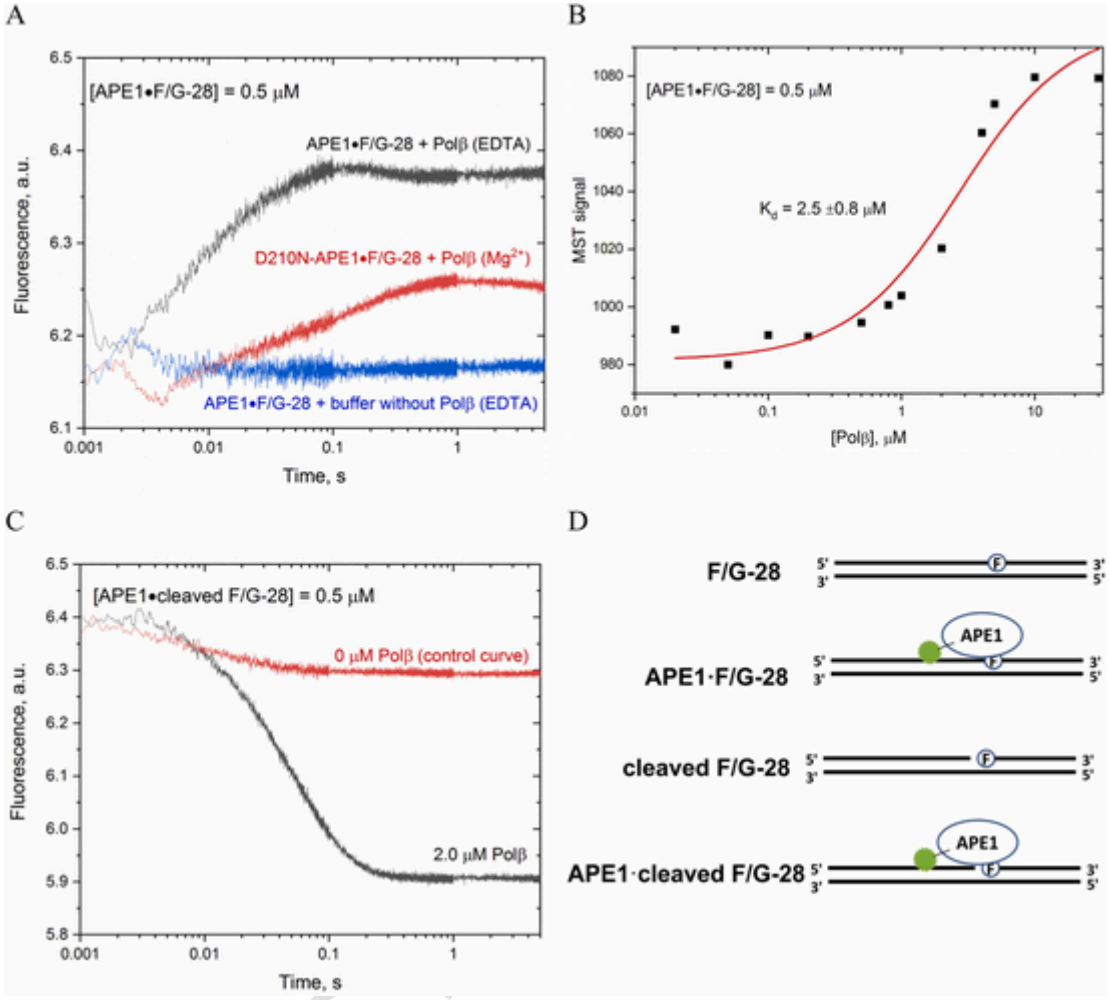

Fig. 6. (A) The interaction of the APE1–F/G-28 complex with Polβ. The cleavage of substrate F/G-28 was prevented by means of EDTA-containing binding buffer without Mg^{2+} ions (black curve) or by means of the labeled inactive D210N APE1 mutant (red curve). (B) The MST assay of the binding of Polβ to the APE1–F/G-28 enzyme–substrate complex. (C) The Alexa Fluor 488 fluorescence trace of the interaction of the enzyme–product complex with Polβ. (D) Schematics of the DNA duplex molecules and their complexes with APE1. (For interpretation of the references to color in this figure legend, the reader is referred to the web version of this article.)

We also used fluorescently labeled Δ34-D210N-APE1 to monitor its binding to cleaved F/G-28 DNA (Supplementary Fig. S14B). Our data suggest that the NΔ34 deletion leads to some decrease in the strength of the enzyme–product association. This result is consistent with previously hypothesized facilitation of enzyme–product dissociation by the NΔ33 deletion in APE1 [99].

4. Conclusion

In this work, we prepared WT and mutant APE1 proteins labeled with the Alexa Fluor 488 fluorophore. It was found that the Alexa Fluor 488 label gets attached mainly to a single residue on the protein's surface, namely Cys99. This label in APE1 was shown to change its fluorescence intensity during the interaction between APE1 and an F-site–containing oligodeoxynucleotide. The changes in Alexa Fluor 488 fluorescence intensity can be assigned to stages of the enzyme–DNA interaction. A comparison of intramolecular conformational changes of the enzyme (own Trp residues of the enzyme), intramolecular changes of the DNA duplex (FRET detection of the FAM/BHQ1 pair in model DNA), and Alexa Fluor 488 fluorescence behavior suggests that the first phase of Alexa Fluor 488 fluorescence change corresponds to the enzyme–DNA binding and to the formation of a catalytically competent complex. The second phase of the Alexa Fluor 488 fluorescence traces was ascribed to DNA cleavage and product release steps.

Interaction of labeled APE1 with a 13-nt, 17-nt, or 28-nt model F-site–containing substrate was examined by Alexa Fluor 488 fluorescence monitoring. The results suggest that after APE1 cleaves oligodeoxynucleotide F/G-17, the generated short 5-nt oligonucleotide dissociates immediately from the enzyme–product complex, but the other parts of the product of the endonucleolytic reaction remain mostly bound to the APE1. By contrast, F/G-28 cleaved by APE1 dissociates from the enzyme poorly and remains mainly in the complex with APE1.

Using fluorescently labeled APE1 in combination with a stopped-flow fluorescence assay, we detected specific DNA-mediated interactions between APE1 and Polβ. Polβ was found to stimulate both i) the binding of APE1 to an F-site–containing duplex oligodeoxynucleotide with the formation of the catalytically competent complex and ii) the dissociation of APE1 from its product. These findings confirm that the passing-the-baton model [44] is applicable to the coordination of BER processes by Polβ via APE1 and explain the previously documented [50] stimulation of APE1 by Polβ.

Funding

This work was supported partially by the Russian Federal Ministry of Science and Higher Education (project No. 121031300041-4) to O.S.F. and N.A.K., by Electricité de France (RB 2020-02 and RB 2021-05) to M.S., a grant from the Science Committee of the Ministry of Education and Science of the Republic of Kazakhstan (No. AP08856811) to M.S., and Fondation ARC (PJA-2021060003796) to A.A.I. The part of the work involving the stopped-flow analysis was specifically funded by Russian Science Foundation grant No. 21-64-00017.

CRediT authorship contribution statement

Artemiy S. Bakman : Data curation, Formal analysis, Investigation, Methodology. **Aleksandra A. Kuznetsova :** Investigation, Methodology, Validation. **Lyudmila V. Yanshole :** Data curation, Formal analysis, Investigation, Methodology. **Alexander A. Ishchenko :** Investigation, Methodology, Funding acquisition. **Murat Saparbaev :** Investigation, Methodology, Funding acquisition. **Olga S. Fedorova :** Resources, Writing – original draft, Writing – review & editing. **Nikita A. Kuznetsov :** Funding acquisition, Conceptualization, Supervision, Validation, Visualization, Writing – original draft, Writing – review & editing.

Conflict of interest

The authors declare that they have no conflicts of interest.

Data availability

Data will be made available on request.

Appendix A. Supporting information

Supplementary data associated with this article can be found in the online version at doi:10.1016/j.dnarep.2023.103450.

References

[1] E.C. Friedberg, G.C. Walker, W. Siede, R.D. Wood, R.A. Schultz, T. Ellenberger, DNA Repair and Mutagenesis, ASM Press, Washington, 2005, https://doi.org/10.1128/9781555816704.
[2] T. Lindahl, S. Ljungquist, Apurinic and apyrimidinic sites in DNA, Basic Life Sci. 5 A (1975) 31–38, https://doi.org/10.1007/978-1-4684-2895-7_5.
[3] B.N. Ames, Endogenous oxidative DNA damage, aging, and cancer, Free Radic. Res. 7 (1989) 121–128, https://doi.org/10.3109/10715768909087933.
[4] B.N. Ames, L.S. Gold, Endogenous mutagens and the causes of aging and cancer, Mutat. Res. Fundam. Mol. Mech. Mutagen 250 (1991) 3–16, https://doi.org/10.1016/0027-5107(91)90157-J.
[5] M.S. Cooke, M.D. Evans, M. Dizdaroglu, J. Lunec, Oxidative DNA damage: mechanisms, mutation, and disease, FASEB J. 17 (2003) 1195–1214, https://doi.org/10.1096/fj.02-0752rev.
[6] A.A. Kuznetsova, D.G. Knorre, O.S. Fedorova, Oxidation of DNA and its components with reactive oxygen species, Russ. Chem. Rev. 78 (2009) 659–678, https://doi.org/10.1070/rc2009v078n07abeh004038.
[7] W.K. Lutz, Endogenous genotoxic agents and processes as a basis of spontaneous carcinogenesis, Mutat. Res. Genet. Toxicol. 238 (1990) 287–295, https://doi.org/10.1016/0165-1110(90)90020-C.
[8] T. Lindahl, Instability and decay of the primary structure of DNA, Nature 362 (1993) 709–715, https://doi.org/10.1038/362709a0.
[9] B. Sedgwick, P.A. Bates, J. Paik, S.C. Jacobs, T. Lindahl, Repair of alkylated DNA: recent advances, DNA Repair 6 (2007) 429–442, https://doi.org/10.1016/j.dnarep.2006.10.005.
[10] N. Kondo, A. Takahashi, K. Ono, T. Ohnishi, DNA damage induced by alkylating agents and repair pathways, J. Nucleic Acids 2010 (2010) 543531, https://doi.org/10.4061/2010/543531.
[11] P.S. Thompson, D. Cortez, New insights into abasic site repair and tolerance, DNA Repair 90 (2020) 102866, https://doi.org/10.1016/j.dnarep.2020.102866.
[12] R.L. Swanson, N.J. Morey, P.W. Doetsch, S. Jinks-Robertson, Overlapping specificities of base excision repair, nucleotide excision repair, recombination, and translesion synthesis pathways for dna base damage in Saccharomyces cerevisiae, Mol. Cell. Biol. 19 (1999) 2929–2935, https://doi.org/10.1128/mcb.19.4.2929.
[13] S. Adar, L. Izhar, A. Hendel, N. Geacintov, Z. Livneh, Repair of gaps opposite lesions by homologous recombination in mammalian cells, Nucleic Acids Res. 37 (2009) 5737–5748, https://doi.org/10.1093/nar/gkp632.
[14] D. Cortez, Replication-coupled DNA repair, Mol. Cell. 74 (2019) 866–876, https://doi.org/10.1016/j.molcel.2019.04.027.
[15] K.P. Bhat, D. Cortez, RPA and RAD51: fork reversal, fork protection, and genome stability, Nat. Struct. Mol. Biol. 25 (2018) 446–453, https://doi.org/10.1038/s41594-018-0075-z.
[16] R. Zellweger, D. Dalcher, K. Mutreja, M. Berti, J.A. Schmid, R. Herrador, A. Vindigni, M. Lopes, Rad51-mediated replication fork reversal is a global response to genotoxic treatments in human cells, J. Cell Biol. 208 (2015) 563–579, https://doi.org/10.1083/jcb.201406099.
[17] M.P. Golinelli, N.H. Chmiel, S.S. David, Site-directed mutagenesis of the cysteine ligands to the [4Fe-4S] cluster of Escherichia coli MutY, Biochemistry 38 (1999) 6997–7007, https://doi.org/10.1021/bi982300n.
[18] K.K.L. Chan, Q.M. Zhang, G.L. Dianov, Base excision repair fidelity in normal and cancer cells, Mutagenesis 21 (2006) 173–178, https://doi.org/10.1093/mutage/gel020.
[19] C.G. Marsden, J.A. Dragon, S.S. Wallace, J.B. Sweasy, Base excision repair variants in cancer, Methods Enzymol. (2017) 119–157, https://doi.org/10.1016/bs.mie.2017.03.003.
[20] L. Gros, M.K. Saparbaev, J. Laval, Enzymology of the repair of free radicals-induced DNA damage, Oncogene 21 (2002) 8905–8925, https://doi.org/10.1038/sj.onc.1206005.
[21] E. Matta, U. Aliyaskarova, A.A. Kuznetsova, B.T. Matkarimov, O.S. Fedorova, N.A. Kuznetsov, A.A. Ishchenko, M. Saparbaev, Chapter 11. Alternative DNA Repair Pathways to Handle Complex DNA Damage Generated by Oxidative Stress and Anticancer Drugs, in: 2020, 249–278. https://doi.org/10.1039/9781839160769–00249.
[22] G.L. Dianov, U. Hübscher, Mammalian base excision repair: the forgotten archangel, Nucleic Acids Res. 41 (2013) 3483–3490, https://doi.org/10.1093/nar/gkt076.
[23] S.S. Wallace, Base excision repair: a critical player in many games, DNA Repair 19 (2014) 14–26, https://doi.org/10.1016/j.dnarep.2014.03.030.
[24] P.W. Doetsch, R.P. Cunningham, The enzymology of apurinic/apyrimidinic endonucleases, Mutat. Res. Repair. 236 (1990) 173–201, https://doi.org/10.1016/0921-8777(90)90004-O.
[25] D.W. Mosbaugh, S.E. Bennett, Uracil-Excision DNA Repair, Prog. Nucleic Acid. Res. Mol. Biol. 48 (1994) 315–370, https://doi.org/10.1016/S0079-6603(08)60859-4.
[26] M. Li, D.M. Wilson, Human Apurinic/Apyrimidinic endonuclease 1, Antioxid. Redox Signal. 20 (2014) 678–707, https://doi.org/10.1089/ars.2013.5492.
[27] A.M. Whitaker, B.D. Freudenthal, APE1: a skilled nucleic acid surgeon, DNA Repair 71 (2018) 93–100, https://doi.org/10.1016/j.dnarep.2018.08.012.
[28] Y. Matsumoto, K. Kim, Excision of deoxyribose phosphate residues by DNA polymerase β during DNA repair, Science 269 (1995) 699–702, https://doi.org/10.1126/science.7624801.
[29] C.E. Piersen, R. Prasad, S.H. Wilson, R.S. Lloyd, Evidence for an imino intermediate in the DNA polymerase β deoxyribose phosphate excision reaction, J. Biol. Chem. 271 (1996) 17811–17815, https://doi.org/10.1074/jbc.271.30.17811.
[30] D.K. Srivastava, B.J. Vande Berg, R. Prasad, J.T. Molina, W.A. Beard, A.E. Tomkinson, S.H. Wilson, Mammalian abasic site base excision repair: identification of the reaction sequence and rate-determining steps, J. Biol. Chem. 273 (1998) 21203–21209, https://doi.org/10.1074/jbc.273.33.21203.
[31] A. Kumar, A.J. Reed, W.J. Zahurancik, S.M. Daskalova, S.M. Hecht, Z. Suo, Interlocking activities of DNA polymerase β in the base excision repair pathway, Proc. Natl. Acad. Sci. USA 119 (2022), https://doi.org/10.1073/pnas.2118940119.
[32] W.A. Beard, S.H. Wilson, Structure and mechanism of DNA polymerase β, Biochemistry 53 (2014) 2768–2780, https://doi.org/10.1021/bi500139h.
[33] G. Dianov, A. Price, T. Lindahl, Generation of single-nucleotide repair patches following excision of uracil residues from DNA, Mol. Cell. Biol. 12 (1992) 1605–1612, https://doi.org/10.1128/mcb.12.4.1605-1612.1992.
[34] Y. Matsumoto, K. Kim, D.F. Bogenhagen, Proliferating cell nuclear antigen-dependent abasic site repair in Xenopus laevis oocytes: an alternative pathway of base excision DNA repair, Mol. Cell. Biol. 14 (1994) 6187–6197, https://doi.org/10.1128/mcb.14.9.6187-6197.1994.
[35] I.I. Dianova, K.M. Sleeth, S.L. Allinson, J.L. Parsons, C. Breslin, K.W. Caldecott, G.L. Dianov, XRCC1-DNA polymerase β interaction is required for efficient base excision repair, Nucleic Acids Res. 32 (2004) 2550–2555, https://doi.org/10.1093/nar/gkh567.
[36] Z.K. Nazarkina, S.N. Khodyreva, S. Marsin, O.I. Lavrik, J.P. Radicella, XRCC1 interactions with base excision repair DNA intermediates, DNA Repair 6 (2007) 254–264, https://doi.org/10.1016/j.dnarep.2006.10.002.
[37] A.E. Vidal, S. Boiteux, I.D. Hickson, J.P. Radicella, XRCC1 coordinates the initial and late stages of DNA abasic site repair through protein-protein interactions, EMBO J. 20 (2001) 6530–6539, https://doi.org/10.1093/emboj/20.22.6530.
[38] A. Campalans, S. Marsin, Y. Nakabeppu, T.R. O'Connor, S. Boiteux, J.P. Radicella, XRCC1 interactions with multiple DNA glycosylases: a model for its recruitment to base excision repair, DNA Repair 4 (2005) 826–835, https://doi.org/10.1016/J.DNAREP.2005.04.014.
[39] A. Campalans, E. Moritz, T. Kortulewski, D. Biard, B. Epe, J.P. Radicella, Interaction with OGG1 is required for efficient recruitment of XRCC1 to base excision repair and maintenance of genetic stability after exposure to oxidative stress, Mol. Cell. Biol. 35 (2015) 1648–1658, https://doi.org/10.1128/

mcb.00134-15.
[40] S. Marsin, A.E. Vidal, M. Sossou, J. Ménissier-De Murcia, F. Le Page, S. Boiteux, G. De Murcia, J.P. Radicella, Role of XRCC1 in the coordination and stimulation of oxidative DNA damage repair initiated by the DNA glycosylase hOGG1, J. Biol. Chem. 278 (2003) 44068–44074, https://doi.org/10.1074/jbc.M306160200.
[41] D.S. Levin, A.E. McKenna, T.A. Motycka, Y. Matsumoto, A.E. Tomkinson, Interaction between PCNA and DNA ligase I is critical for joining of Okazaki fragments and long-patch base-excision repair, Curr. Biol. 10 (2000) 919–922, https://doi.org/10.1016/S0960-9822(00)00619-9.
[42] R. Gary, K. Kim, H.L. Cornelius, M.S. Park, Y. Matsumoto, Proliferating cell nuclear antigen facilitates excision in long-patch base excision repair, J. Biol. Chem. 274 (1999) 4354–4363, https://doi.org/10.1074/jbc.274.7.4354.
[43] N.A. Moor, O.I. Lavrik, Protein–protein interactions in DNA base excision repair, Biochemistry 83 (2018) 411–422, https://doi.org/10.1134/S0006297918040120.
[44] R. Prasad, W.A. Beard, V.K. Batra, Y. Liu, D.D. Shock, S.H. Wilson, A review of recent experiments on step-to-step "hand-off" of the DNA intermediates in mammalian base excision repair pathways, Mol. Biol. 45 (2011) 536–550, https://doi.org/10.1134/S0026893311040091.
[45] Y.-J. Kim, D.M. Wilson III, Overview of base excision repair biochemistry, Curr. Mol. Pharmacol. 5 (2011) 3–13, https://doi.org/10.2174/1874467211205010003.
[46] S.H. Wilson, T.A. Kunkel, Passing the baton in base excision repair, Nat. Struct. Biol. 7 (2000) 176–178, https://doi.org/10.1038/73260.
[47] K.W. Caldecott, Single-strand break repair and genetic disease, Nat. Rev. Genet. 9 (2008) 619–631, https://doi.org/10.1038/nrg2380.
[48] J.L. Parsons, G.L. Dianov, Co-ordination of base excision repair and genome stability, DNA Repai 12 (2013) 326–333, https://doi.org/10.1016/j.dnarep.2013.02.001.
[49] A.V. Endutkin, A.V. Yudkina, V.S. Sidorenko, D.O. Zharkov, Transient protein–protein complexes in base excision repair, J. Biomol. Struct. Dyn. 37 (2019) 4407–4418, https://doi.org/10.1080/07391102.2018.1553741.
[50] O.A. Kladova, I.V. Alekseeva, M. Saparbaev, O.S. Fedorova, N.A. Kuznetsov, Modulation of the apurinic/apyrimidinic endonuclease activity of human APE1 and of its natural polymorphic variants by base excision repair proteins, Int. J. Mol. Sci. 21 (2020) 1–15, https://doi.org/10.3390/ijms21197147.
[51] O.A. Kladova, M. Bazlekowa-Karaban, S. Baconnais, O. Piétrement, A.A. Ishchenko, B.T. Matkarimov, D.A. Iakovlev, A. Vasenko, O.S. Fedorova, E. Le Cam, B. Tudek, N.A. Kuznetsov, M. Saparbaev, The role of the N-terminal domain of human apurinic/apyrimidinic endonuclease 1, APE1, in DNA glycosylase stimulation, DNA Repair 64 (2018) 10–25, https://doi.org/10.1016/j.dnarep.2018.02.001.
[52] D.M. Wilson, D. Barsky, The major human abasic endonuclease: formation, consequences and repair of abasic lesions in DNA, Mutat. Res. DNA Repair 485 (2001) 283–307, https://doi.org/10.1016/S0921-8777(01)00063-5.
[53] B. Demple, J.S. Sung, Molecular and biological roles of Ape1 protein in mammalian base excision repair, DNA Repair (2005) 1442–1449, https://doi.org/10.1016/j.dnarep.2005.09.004.
[54] B. Kavli, O. Sundheim, M. Akbari, M. Otterlei, H. Nilsen, F. Skorpen, P.A. Aas, L. Hagen, H.E. Krokan, G. Slupphaug, hUNG2 is the major repair enzyme for removal of uracil from U:A matches, U:G mismatches, and U in single-stranded DNA, with hSMUG1 as a broad specificity backup, J. Biol. Chem. 277 (2002) 39926–39936, https://doi.org/10.1074/jbc.M207107200.
[55] S.S. Parikh, C.D. Mol, G. Slupphaug, S. Bharati, H.E. Krokan, J.A. Tainer, Base excision repair initiation revealed by crystal structures and binding kinetics of human uracil-DNA glycosylase with DNA, EMBO J. 17 (1998) 5214–5226, https://doi.org/10.1093/emboj/17.17.5214.
[56] T.R. Waters, P. Gallinari, J. Jiricnyl, P.F. Swann, Human thymine DNA glycosylase binds to apurinic sites in DNA but is displaced by human apurinic endonuclease 1, J. Biol. Chem. 274 (1999) 67–74, https://doi.org/10.1074/jbc.274.1.67.
[57] C.V. Privezentzev, M. Saparbaev, J. Laval, The HAP1 protein stimulates the turnover of human mismatch-specific thymine-DNA-glycosylase to process 3,N4-ethenocytosine residues, Mutat. Res. Fundam. Mol. Mech. Mutagen 480–481 (2001) 277–284, https://doi.org/10.1016/S0027-5107(01)00186-5.
[58] M.E. Fitzgerald, A.C. Drohat, Coordinating the initial steps of base excision repair: apurinic/apyrimidinic endonuclease 1 actively stimulates thymine DNA glycosylase by disrupting the product complex, J. Biol. Chem. 283 (2008) 32680–32690, https://doi.org/10.1074/jbc.M805504200.
[59] R.L. Maher, A.C. Vallur, J.A. Feller, L.B. Bloom, Slow base excision by human alkyladenine DNA glycosylase limits the rate of formation of AP sites and AP endonuclease 1 does not stimulate base excision, DNA Repair 6 (2007) 71–81, https://doi.org/10.1016/j.dnarep.2006.09.001.
[60] M.R. Baldwin, P.J. O'Brien, Human AP endonuclease 1 stimulates multiple-turnover base excision by alkyladenine DNA glycosylase, Biochemistry 48 (2009) 6022–6033, https://doi.org/10.1021/bi900517y.
[61] P.J. Luncsford, B.A. Manvilla, D.N. Patterson, S.S. Malik, J. Jin, B.J. Hwang, R. Gunther, S. Kalvakolanu, L.J. Lipinski, W. Yuan, W. Lu, A.C. Drohat, A.L. Lu, E.A. Toth, Coordination of MYH DNA glycosylase and APE1 endonuclease activities via physical interactions, DNA Repair 12 (2013) 1043–1052, https://doi.org/10.1016/j.dnarep.2013.09.007.
[62] H. Yang, W.M. Clendenin, D. Wong, B. Demple, M.M. Slupska, J.H. Chiang, J.H. Miller, Enhanced activity of adenine-DNA glycosylase (Myh) by apurinic/apyrimidinic endonuclease (Ape1) in mammalian base excision repair of an A/GO mismatch, Nucleic Acids Res. 29 (2001) 743–752, https://doi.org/10.1093/nar/29.3.743.
[63] M.A. Pope, S.L. Porello, S.S. David, Escherichia coli apurinic-apyrimidinic endonucleases enhance the turnover of the adenine glycosylase MutY with G:A substrates, J. Biol. Chem. 277 (2002) 22605–22615, https://doi.org/10.1074/jbc.M203037200.
[64] A. Parker, Y. Gu, W. Mahoney, S.H. Lee, K.K. Singh, A.L. Lu, Human homolog of the MutY repair protein (hMYH) physically interacts with proteins involved in long patch DNA base excision repair, J. Biol. Chem. 276 (2001) 5547–5555, https://doi.org/10.1074/jbc.M008463200.
[65] J.W. Hill, T.K. Hazra, T. Izumi, S. Mitra, Stimulation of human 8-oxoguanine-DNA glycosylase by AP-endonuclease: potential coordination of the initial steps in base excision repair, Nucleic Acids Res. 29 (2001) 430–438, https://doi.org/10.1093/nar/29.2.430.
[66] V.S. Sidorenko, G.A. Nevinsky, D.O. Zharkov, Mechanism of interaction between human 8-oxoguanine-DNA glycosylase and AP endonuclease, DNA Repair 6 (2007) 317–328, https://doi.org/10.1016/j.dnarep.2006.10.022.
[67] A.E. Vidal, I.D. Hickson, S. Boiteux, J.P. Radicella, Mechanism of stimulation of the DNA glycosylase activity of hOGG1 by the major human AP endonuclease: bypass of the AP lyase activity step, Nucleic Acids Res. 29 (2001) 1285–1292, https://doi.org/10.1093/nar/29.6.1285.
[68] A. Esadze, G. Rodriguez, S.L. Cravens, J.T. Stivers, AP-endonuclease 1 accelerates turnover of human 8-oxoguanine DNA glycosylase by preventing retrograde binding to the abasic-site product, Biochemistry 56 (2017) 1974–1986, https://doi.org/10.1021/acs.biochem.7b00017.
[69] A.T. Raper, B.A. Maxwell, Z. Suo, Dynamic processing of a common oxidative DNA lesion by the first two enzymes of the base excision repair pathway, J. Mol. Biol. 433 (2021) 166811, https://doi.org/10.1016/j.jmb.2021.166811.
[70] R.A.O. Bennett, D.M. Wilson, D. Wong, B. Demple, Interaction of human apurinic endonuclease and DNA polymerase β in the base excision repair pathway, Proc. Natl. Acad. Sci. USA 94 (1997) 7166–7169, https://doi.org/10.1073/pnas.94.14.7166.
[71] D. Wong, B. Demple, Modulation of the 5′-deoxyribose-5-phosphate lyase and DNA synthesis activities of mammalian DNA polymerase β by apurinic/apyrimidinic endonuclease 1, J. Biol. Chem. 279 (2004) 25268–25275, https://doi.org/10.1074/jbc.M400804200.
[72] N. Moor, I. Vasil'eva, O. Lavrik, Functional role of N-terminal extension of human ap endonuclease 1 in coordination of base excision dna repair via protein–protein interactions, Int. J. Mol. Sci. 21 (2020) 3122, https://doi.org/10.3390/ijms21093122.
[73] N.A. Moor, I.A. Vasil'eva, R.O. Anarbaev, A.A. Antson, O.I. Lavrik, Quantitative characterization of protein-protein complexes involved in base excision DNA repair, Nucleic Acids Res. 43 (2015) 6009–6022, https://doi.org/10.1093/nar/gkv569.
[74] I.A. Vasil'eva, R.O. Anarbaev, N.A. Moor, O.I. Lavrik, Dynamic light scattering study of base excision DNA repair proteins and their complexes, Biochim. Biophys. Acta Proteins Proteom. 1867 (2019) 297–305, https://doi.org/10.1016/j.bbapap.2018.10.009.
[75] Y. Liu, R. Prasad, W.A. Beard, P.S. Kedar, E.W. Hou, D.D. Shock, S.H. Wilson, Coordination of steps in single-nucleotide base excision repair mediated by apurinic/apyrimidinic endonuclease 1 and DNA polymerase β, J. Biol. Chem. 282 (2007) 13532–13541, https://doi.org/10.1074/jbc.M611295200.
[76] O.S. Alekseeva, I.V. Davletgildeeva, A.T. Arkova, O.V. Kuznetsov, N.A. Fedorova, The impact of single-nucleotide polymorphisms of human apurinic/apyrimidinic endonuclease 1 on specific DNA binding and catalysis, Biochimie 163 (2019) 73–83, https://doi.org/10.1016/j.biochi.2019.05.015.
[77] A.A. Kuznetsova, N.A. Kuznetsov, A.A. Ishchenko, M.K. Saparbaev, O.S. Fedorova, Pre-steady-state fluorescence analysis of damaged DNA transfer from human DNA glycosylases to AP endonuclease APE1, Biochim. Biophys. Acta Gen. Subj. 1840 (2014) 3042–3051, https://doi.org/10.1016/j.bbagen.2014.07.016.
[78] A.D. Miroshnikova, A.A. Kuznetsova, N.A. Kuznetsov, O.S. Fedorova, Thermodynamics of damaged DNA binding and catalysis by human AP endonuclease 1, Acta Nat. 8 (2016) 103–110, https://doi.org/10.32607/20758251-2016-8-1-103-110.
[79] O.A. Krumkacheva, G.Y. Shevelev, A.A. Lomzov, N.S. Dyrkheeva, A.A. Kuzhelev, V.V. Koval, V.M. Tormyshev, Y.F. Polienko, M.V. Fedin, D.V. Pyshnyi, O.I. Lavrik, E.G. Bagryanskaya, DNA complexes with human apurinic/apyrimidinic endonuclease 1: structural insights revealed by pulsed dipolar EPR with orthogonal spin labeling, Nucleic Acids Res. 47 (2019) 7767–7780, https://doi.org/10.1093/nar/gkz620.
[80] D.A. Yakovlev, A.A. Kuznetsova, O.S. Fedorova, N.A. Kuznetsov, Search for modified DNA sites with the human methyl-CpG-binding enzyme MBD4, Acta Nat. 9 (2017) 26–37, https://doi.org/10.32607/20758251-2017-9-1-88-98.
[81] A.A. Kuznetsova, D.A. Iakovlev, I.V. Misovets, A.A. Ishchenko, M.K. Saparbaev, N.A. Kuznetsov, O.S. Fedorova, Pre-steady-state kinetic analysis of damage recognition by human single-strand selective monofunctional uracil-DNA glycosylase SMUG1, Mol. Biosyst. 13 (2017) 2638–2649, https://doi.org/10.1039/c7mb00457e.
[82] O.A. Kladova, A.A. Kuznetsova, O.S. Fedorova, N.A. Kuznetsov, Mutational and kinetic analysis of lesion recognition by Escherichia coli endonuclease VIII, Genes 8 (2017) 1–13, https://doi.org/10.3390/genes8050140.
[83] N.A. Timofeyeva, V.V. Koval, D.G. Knorre, D.O. Zharkov, M.K. Saparbaev, A.A. Ishchenko, O.S. Fedorova, Conformational dynamics of human ap endonuclease in base excision and nucleotide incision repair pathways, J. Biomol. Struct. Dyn. 26 (2009) 637–652, https://doi.org/10.1080/07391102.2009.10507278.
[84] L.Y. Kanazhevskaya, V.V. Koval, D.O. Zharkov, P.R. Strauss, O.S. Fedorova, Conformational transitions in human AP endonuclease 1 and its active site mutant during abasic site repair, Biochemistry 49 (2010) 6451–6461, https://doi.org/

10.1021/bi100769k.
[85] A.D. Miroshnikova, A.A. Kuznetsova, Y.N. Vorobjev, N.A. Kuznetsov, O.S. Fedorova, Effects of mono- and divalent metal ions on DNA binding and catalysis of human apurinic/apyrimidinic endonuclease 1, Mol. Biosyst. 12 (2016) 1527–1539, https://doi.org/10.1039/c6mb00128a.
[86] L.Y. Kanazhevskaya, V.V. Koval, Y.N. Vorobjev, O.S. Fedorova, Conformational dynamics of abasic DNA upon interactions with AP endonuclease 1 revealed by stopped-flow fluorescence analysis, Biochemistry 51 (2012) 1306–1321, https://doi.org/10.1021/bi201444m.
[87] I.V. Alekseeva, A.A. Kuznetsova, A.S. Bakman, O.S. Fedorova, N.A. Kuznetsov, The role of active-site amino acid residues in the cleavage of DNA and RNA substrates by human apurinic/apyrimidinic endonuclease APE1, Biochim. Biophys. Acta Gen. Subj. 1864 (2020), https://doi.org/10.1016/j.bbagen.2020.129718.
[88] R.L. Maher, L.B. Bloom, Pre-steady-state kinetic characterization of the AP endonuclease activity of human AP endonuclease 1, J. Biol. Chem. 282 (2007) 30577–30585, https://doi.org/10.1074/jbc.M704341200.
[89] K.M. Schermerhorn, S. Delaney, Transient-state kinetics of apurinic/apyrimidinic (AP) endonuclease 1 acting on an authentic AP site and commonly used substrate analogs: the effect of diverse metal ions and base mismatches, Biochemistry 52 (2013) 7669–7677, https://doi.org/10.1021/bi401218r.
[90] L. Gros, A.A. Ishchenko, H. Ide, R.H. Elder, M.K. Saparbaev, The major human AP endonuclease (Ape1) is involved in the nucleotide incision repair pathway, Nucleic Acids Res. 32 (2004) 73–81, https://doi.org/10.1093/nar/gkh165.
[91] P. Prorok, D. Alili, C. Saint-Pierre, D. Gasparutto, D.O. Zharkov, A.A. Ishchenko, B. Tudek, M.K. Saparbaev, Uracil in duplex DNA is a substrate for the nucleotide incision repair pathway in human cells, Proc. Natl. Acad. Sci. USA 110 (2013) E3695–E3703, https://doi.org/10.1073/pnas.1305624110.
[92] A.A. Kuznetsova, A.G. Matveeva, A.D. Milov, Y.N. Vorobjev, S.A. Dzuba, O.S. Fedorova, N.A. Kuznetsov, Substrate specificity of human apurinic/apyrimidinic endonuclease APE1 in the nucleotide incision repair pathway, Nucleic Acids Res. 46 (2018) 11454–11465, https://doi.org/10.1093/nar/gky912.
[93] Y. Masuda, R.A.O. Bennett, B. Demple, Rapid dissociation of human apurinic endonuclease (Ape1) from incised DNA induced by magnesium, J. Biol. Chem. 273 (1998) 30360–30365, https://doi.org/10.1074/jbc.273.46.30360.
[94] C.D. Mol, T. Izumi, S. Mitra, J.A. Tainer, DNA-bound structures and mutants reveal abasic DNA binding by APE1 DNA repair and coordination, Nature 403 (2000) 451–456, https://doi.org/10.1038/35000249.
[95] S.R. Peddi, R. Chattopadhyay, C.V.V. Naidu, T. Izumi, The human apurinic/apyrimidinic endonuclease-1 suppresses activation of poly(adp-ribose) polymerase-1 induced by DNA single strand breaks, Toxicology 224 (2006) 44–55, https://doi.org/10.1016/j.tox.2006.04.025.
[96] I.V. Alekseeva, A.S. Bakman, Y.N. Vorobjev, O.S. Fedorova, N.A. Kuznetsov, Role of ionizing amino acid residues in the process of DNA binding by human AP endonuclease 1 and in Its catalysis, J. Phys. Chem. B 123 (2019) 9546–9556, https://doi.org/10.1021/acs.jpcb.9b07150.
[97] E.K. Dimitriadis, R. Prasad, M.K. Vaske, L. Chen, A.E. Tomkinson, M.S. Lewis, S.H. Wilson, Thermodynamics of human DNA ligase I trimerization and association with DNA polymerase β, J. Biol. Chem. 273 (1998) 20540–20550, https://doi.org/10.1074/jbc.273.32.20540.
[98] C. Vascotto, D. Fantini, M. Romanello, L. Cesaratto, M. Deganuto, A. Leonardi, J.P. Radicella, M.R. Kelley, C. D'Ambrosio, A. Scaloni, F. Quadrifoglio, G. Tell, APE1/Ref-1 Interacts with NPM1 within Nucleoli and Plays a Role in the rRNA Quality Control Process, Mol. Cell. Biol. 29 (2009) 1834–1854, https://doi.org/10.1128/mcb.01337-08.
[99] D. Fantini, C. Vascotto, D. Marasco, C. D'Ambrosio, M. Romanello, L. Vitagliano, C. Pedone, M. Poletto, L. Cesaratto, F. Quadrifoglio, A. Scaloni, J.P. Radicella, G. Tell, Critical lysine residues within the overlooked N-terminal domain of human APE1 regulate its biological functions, Nucleic Acids Res. 38 (2010) 8239–8256, https://doi.org/10.1093/nar/gkq691.
[100] O.A. Kladova, M. Bazlekowa-Karaban, S. Baconnais, O. Piétrement, A.A. Ishchenko, B.T. Matkarimov, D.A. Iakovlev, A. Vasenko, O.S. Fedorova, E. Le Cam, B. Tudek, N.A. Kuznetsov, M. Saparbaev, The role of the N-terminal domain of human apurinic/apyrimidinic endonuclease 1, APE1, in DNA glycosylase stimulation, DNA Repair 64 (2018) 10–25, https://doi.org/10.1016/j.dnarep.2018.02.001.
[101] M. De Falco, N. Komaniecka, M. Porras, L. Cairn, J. Ander Santas, N. Ferreiro, J. Carlos Penedo, S. Bañuelos, Conformational rearrangements regulating the DNA repair protein APE1, Int. J. Mol. Sci. 23 (2022) 8015, https://doi.org/10.3390/IJMS23148015.